Controlled fabrication of $BiFeO_3$ uniform nanoparticles and their magnetic behaviors

YAN LU[a], JIANKANG LI[a,b*]
[a] *Jiangsu Key Laboratory for Environment Functional Materials, Suzhou University of Science and Technology, Suzhou 215009, China*
[b] *Schools of Mathematics and Physics, Suzhou University of Science and Technology, Suzhou 215009, China*

Uniform $BiFeO_3$ (BFO) nanoparticles was prepared by hydrothermal synthesis method using $Fe(NO_3)_3 \cdot 9H_2O$ and $Bi(NO_3)_3 \cdot 5H_2O$ as the basic raw materials. Studies have shown that pure phase BFO nanoparticles could be prepared successfully under hydrothermal conditions of reaction temperature of 200 °C and time of 24 h. Particle shapes of the powder are uniform as well as the sizes, which have not yet been reported, and remanent magnetization of which reaches 0.054 emu/g. Temperature dependences of the saturation magnetization curve was measured, from which Curie temperature and Neel temperature of BFO nanoparticles are confirmed, predicting the coupling between the ferromagnetism and ferroelectricity should be strong. Possible formation mechanism of the microcrystal was also proposed.

(Received September 28, 2012; accepted February 20, 2013)

Keywords: Hydrothermal synthesis, $BiFeO_3$, Nanoparticles, Raman

1. Introduction

Multiferroic materials, coexisting of ferroelectric and magnetic orders in a certain range of temperature, have received considerable interest in the past few years due to the fascinating physics properties and potential applications for magnetoelectric devices [1]. As the only multiferroic material of which Curie temperature (1100 K) and Neel temperature (643 K) are above room temperature, BFO receives extensive attention, which makes it one of the candidates for room-temperature ME applications. Beside above-mentioned applications, BFO provides opportunities for potential applications in data storage, spintronics, microelectronic devices and visible-light photocatalyst [2].

On the one hand, as is well known, the properties of materials, such as magnetic, electrical, and optical properties are closely interconnected with crystal structure. So an intensive study of controlled synthesis and self-organization of materials with regular geometrical shapes is significant for developing fundamental physics as well as designing new devices [3]. On the other, the fabrication of pure multiferroic BFO nanoparticles is difficult because of the volatilization of Bi^{2+} ions [4]. In order to overcome these two problems, hydrothermal synthesis is adopted. Among the very many techniques used to prepare BFO nanoparticles, hydrothermal synthesis has its unique advantages such as low annealing temperature, easy operation, no volatilization of Bi^{2+} ions [1], and primarily it is a good method used to prepare different-shaped BFO microcrystal nanoparticles [5], which provides a good way to investigate their morphology and size-dependent chemical and physical properties. Desirable morphologies such as nanocubes, nanotubes, nanowires [6], and well-defined microcrystal have been prepared, structure, magnetic and optical properties of which were observed and analyzed. In this paper, a new well-defined BFO microcrystal nanoparticles was prepared employing hydrothermal process. The crystal structures, morphologies, magnetic properties of the as-prepared material were investigated in detail, and possible formation mechanism for this BFO microcrystal was proposed.

2. Experiments

2.1 Preparation of BFO nanoparticles

BFO nanoparticles were prepared by hydrothermal synthesis. Stoicheometric $Fe(NO_3)_3 \cdot 9H_2O$ and $Bi(NO_3) \cdot 5H_2O$ were dissolved in distilled water. A little amount of nitric acid was added to help dissolve $Bi(NO_3) \cdot 5H_2O$. The mixture was dropped into KOH solution as slowly as possible under magnetic stirring. The final pH, volume equals 14, 80 ml, respectively. Then the solution was dispersed with ultrasonic

processing condition for 30 min. After that, the solution was transferred to a stainless steel Teflon-lined autoclave of 100 mL capacity. The autoclave was sealed and heated at 200 °C for 24 h without shaking or stirring and then cooled to room temperature naturally. The final products were collected by being dried at 70 °C for a period of time before further characterization.

2.2 Characterization

The purity and crystallinity of the sample were characterized by X-ray diffraction (XRD, D8-focus) using Cu Kα radiation. The working voltage and electric current were held at 40 kV and 150 mA, respectively. The morphologies of samples were investigated by scanning electron microscope (SEM) and transmission electron microscopy (TEM). High-resolution transmission electron microscopy (HRTEM) was carried out using a JEOL-2011 instrument with an accelerating voltage of 200 kV. Raman scattering spectra were recorded in backscattering geometry on RM 2000 (Renishaw) with a radiation of Ar^+ laser at 514.5 nm focused over a 5 μm diameter area. The room temperature magnetization-magnetic fields curve (M-H), as well as magnetization-temperature curve (M-H), were tested by vibrating sample magnetometer (VSM).

3. Results and discussion

3.1 The structure of BFO nanoparticles

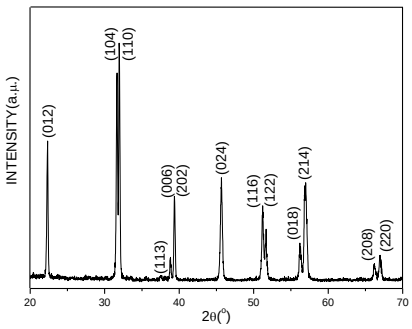

Fig. 1. XRD pattern of BFO nanoparticles.

The phase composition and crystallinity of the product were examined by powder X-ray diffraction (XRD). As shown in Fig. 1, the obvious peak-splitting illustrated that the nanoparticles were distorted perovskite structure. All the reflection peaks in the pattern could be easily indexed to perovskite (space group R3c) BFO (JCPDS card No.86-1518) and no other peaks (such as Fe_2O_3, Bi_2O_3, $Bi_2Fe_4O_9$, etc.) were detected in the pure BFO nanoparticles, demonstrating that well-crystallized single phase BFO nanoparticles could be obtained with this synthesis condition. The mean grain size of nanocrystalline was calculated by Debye-Scherrer formula [7]:

$$D = k\lambda / B\cos\theta$$

where D is the grain size (nm); K is the Scherrer constant whose value is 0.89; B is the full width at half maximum; θ is the diffraction angle; λ equals to the X-ray wavelength (0.154056 nm). The average grain size was about 150 nm calculated with the above formula. In the calculation process a phenomenon that the single grain size (D) corresponded to every diffraction peak under calculation ranges from 89.25 nm to 165.18 nm was found, indicating that the shape of the grains is not spherical, may be rectangular or other irregular shape.

3.2 The morphologies of BFO nanoparticles

The morphology of BFO samples were investigated by SEM, TEM and HRTEM. Typical SEM images of pure BFO nanoparticles were shown in Fig. 2. As is seen from these two photographs that every nanoparticle is rectangular, which exhibits a well-defined cubic morphology with an average particle size of about 150 nm, the length, width, and height of the nanoparticles equal about 250 nm, 100 nm, 70 nm, respectively. The TEM image shown in Fig. 3. (a) matched well with the above SEM images. The morphologies of the nanoparticles, observed for the first time in BFO, have not yet been reported. A corresponding HRTEM image of pure BFO nanoparticles was shown in Fig. 3. (b). The regular spacings of the observed lattice are 0.385 nm and 0.278 nm, corresponded to the (012) and (110) crystal planes of rhombohedral BFO crystal, respectively.

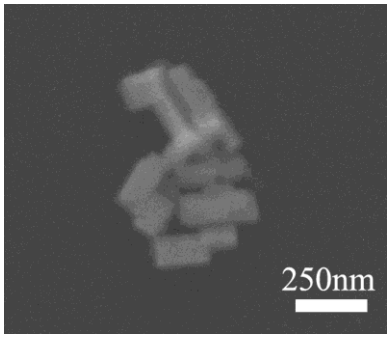

Fig. 2. SEM images of typical BFO nanoparticles.

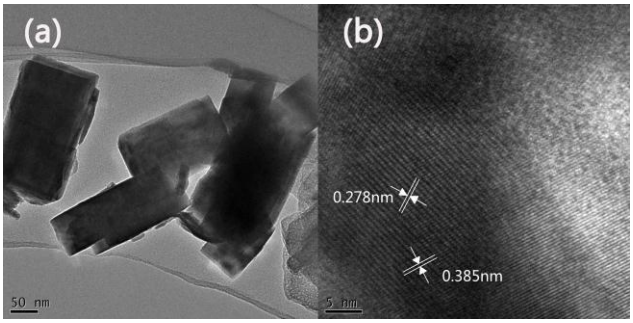

Fig. 3. (a) TEM image of BFO nanoparticles; (b) HRTEM image of BFO nanoparticles

3.3 Formation mechanism of BFO nanoparticles

Here, the possible growth mechanisms of as-prepared nanoparticles were investigated. The formation of BFO nanoparticles was achieved through the following process. First, make large numbers of BFO small crystallites nucleated [8]. As the reaction continued, the morphologies of the particles prepared by different methods may be different. For example, nanoparticles prepared by chemical vapor deposition mostly have a uniform size distribution and spherical shape [9], but using hydrothermal process, some special forms like microcubes and submicrocubes can be successfully synthesized [8].

The growing of structural features is influenced by internal stress and lowest energy principle. Spherical shape is easy to be fabricated by chemical vapor deposition for that the temperature difference from gaseous to solid state reaches at least 2000 °C for a second. Under the circumstances, lowest energy principle plays a critical role when internal stress is comparatively ineffective. But on the contrary, when hydrothermal process is adopted, reaction conditions change slowly, which give rise to the result that internal stress plays a greater part than the lowest energy principle, so microcubes and submicrocubes can grow according to their own lattice parameters in the presence of internal stress. Taking the as-prepared sample as example, large numbers of BFO unit cell nucleate and grow into small seed particles, after which the larger BFO nanoparticles grow gradually following every crystal plane, so the morphology of final product is more or less like BFO unit cell. Therefore, the formation of BFO is believed to follow the Ostwald ripening process [10]. In addition, the morphology of final product is also influenced by pH, additives and so on.

3.4 Raman spectroscopy analysis of BFO nanoparticles

The Raman spectroscopy data of the as-prepared product shown in Fig. 4 are in good consistency with the X-ray diffraction pattern, showing that the nanoparticles are distorted perovskite BFO. Four A_1 modes are marked in the figure, and the arrows represent E modes. The nanoparticles show similar structure to other reported data [11]. The presence of the R3c symmetry is shown by Raman spectroscopy analysis and a small crystalline size is indicated by the bands wide features.

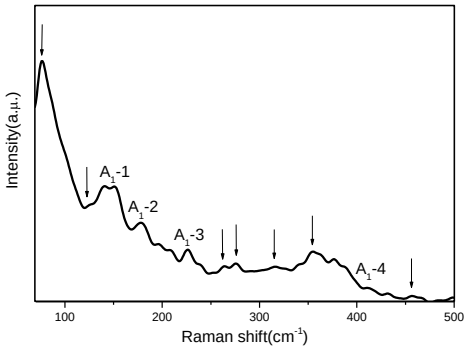

Fig. 4. Raman features of the as-prepared BFO nanoparticles.

3.5 Magnetic properties of BFO nanoparticles

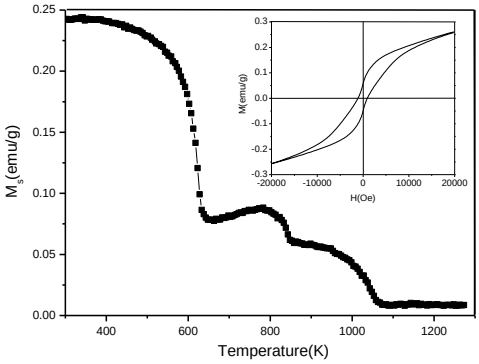

Fig. 5. The room-temperature magnetization-magnetic field (M-H) curve of BFO nanoparticles and temperature dependences of the saturation magnetization curve under 1000 Oe.

As given in Fig. 5, the saturation magnetization - temperature (M-T) curve from 300 to 1200 K of the sample was measured at an applied field of 1000 Oe. Neel temperature (643 K) is confirmed by the turning point at 660 K, which matches well with it. At the ferroelectric transition temperature (1100 K), the M-T curve shows a change as shown in Fig. 5. So the coupling between the ferromagnetism and ferroelectricity should be strong. There could be a phase transition at the turning point of 825 K, which needed further researches.

The room-temperature magnetization-magnetic field (M-H) curve of BFO nanoparticles under the maximum

magnetic field (Hm) of 20 kOe is shown in the illustration of Fig. 5. The values of remnant magnetization (Mr) and coercive field (Hc) of the sample reach 0.054 emu/g and 1026.4 Oe, respectively, which is significantly greater than the previous reports [12], and is different from the linear M-H behavior in bulk BFO [13]. But the magnetic properties of as-prepared product are inferior to which reported by Park et al [14] of 41 nm nanocrystals. It is well known that the wavelength of the incommensurate cycloid spin structure in bulk BFO is 62 nm. As the particle size is more than 62 nm, magnetic properties originated from incommensurate cycloid spin structure cancel each other out and grow smaller, for that the cycloid structure in bulk BFO is partially destroyed.

4. Conclusions

Pure phase BFO nanoparticles were successfully prepared by hydrothermal synthesis method using $Fe(NO_3)_3 \cdot 9H_2O$ and $Bi(NO_3)_3 \cdot 5H_2O$ as the basic raw materials under hydrothermal conditions of reaction temperature of 200 °C and time of 24h. All the reflection peaks in the XRD pattern can be easily indexed to perovskite (space group R3c) BFO (JCPDS card No.86-1518), confirmed by the Raman spectroscopy data without detecting other peaks. Shown in the TEM images, every nanoparticle is rectangular, which exhibits a well-defined cubic morphology with an average particle size of about 150 nm and particle shapes of the powder are uniform as well as the sizes. Possible formation mechanism for the microcrystal was proposed. Remanent magnetization reaches 0.054 emu/g. Curie temperature (1100 K) and Neel temperature (643 K) were confirmed by the temperature dependences of the saturation magnetization curve.

Acknowledgements

This work was supported by the Jiangsu Provincial Natural Science Foundation (No. BK2005039) and the Jiangsu University Natural Science Research Project (No. 05KJB430127).

References

[1] H. R. Liu, Y. X. Sun. J. Phys. D Appl. Phys. **40**, 859 (2007).
[2] M. Kumar, K. L. Yadav, G. D. Varma. Mater. Lett. **62**, 1159 (2008).
[3] D. Chen, J. H. Ye. Adv. Funct. Mater. **18**, 1922 (2008).
[4] J. K. Kim, S. S. Kim, W. J. Kim. Mater. lett. **59**, 4006 (2005).
[5] M. Mo, J. Zeng, X. Liu, W. Yu, S. Zhang, Y. Qian. Adv. Mater. **14**, 1658 (2002).
[6] F. Gao, Y. Yuan, K. F. Wang, X.Y. Chen, F. Chen, J. M. Liu, Z. F. Ren. Appl. Phys. Lett. **89**, 102506 (2006).
[7] H. Wang, J. R. Zhang, J. J. Zhu. J. Cryst. Growth. **233**, 829 (2001).
[8] S. Li, Y. H. Lin, B. P. Zhang, Y. Wang, C. W. Nan. J. Phys. Chem. C **114**, 7 (2010).
[9] J. A. Ayllón, A. Figueras, S. Garelik, L. Spirkova, J. Durand, L. Cot. J. Mater. Sci. Lett. **18**, 16 (1999).
[10] D. Kothari, V. R. Reddy, V. G. Sathe, A. Gupta, A. Banerjee, A. M. Awasthi. J. Mag. Mag. Mater. **320**, 548 (2008).
[11] R. L. Penn, J. F. Banfield. Science **281**, 969 (1998).
[12] F. Gao, X. Chen, K. Yin, S. Dong, Z. Ren, F. Yuan, T. Yu, Z. Zou, J. M. Liu. Adv. Mater. **19**, 2889 (2007).
[13] S. T. Zhang, M. H. Lu, D. Wu, Y. F. Chen, N. B. Ming. Appl. Phys. Lett. **87**, 262907 (2005).
[14] J. L. Mi, T. N. Jensen, M. Christensen, C. Tyrsted, J. E. Jørgensen, B. B. Iversen. Chem. Mater. **23**, 1158 (2011).

*Corresponding author: yanluusts@163.com